Space Communication

In deep space communications, a request for retransmission would take too long.

From: Encyclopedia of Physical Science and Technology (Third Edition), 2003

Related terms:

Planetary Protection, Communication Satellite, European Space Agency, Binary Digit, Radio Communication, Gamma Radiation, X Ray

View all Topics

Communications Satellite Systems

Takashi Iida, Hiromitsu Wakana, in Encyclopedia of Physical Science and Technology (Third Edition), 2003

III.B.1.a Japan–U.S. Trans-Pacific HDR Satellite Communication Experiment

The Trans-Pacific HDR Satellite Communication Experiment has been studied in the JUSTSAP since 1993 as mentioned earlier. Figure 29 shows the final structure of the experimental system configuration. A hybrid construction was employed for the experimental network, comprising the satellite circuits of NASA's experimental ACTS satellite and the INTELSAT satellite (with no rental fees applied), and three interconnected optical fiber networks in Japan, Hawaii, and California. The first phase of the Trans-Pacific HDR Satellite Communication Experiment was successfully conducted for postproduction high-definition video (HDV) transmission via 45 Mbps ATM (asynchronous transfer mode) circuit between Tokyo and California via Hawaii by using ACTS and INTELSAT in March 1997. The objectives of this experiment were to promote cooperation between Japan and the United States in the space communications field, to demonstrate the technological possibilities for constructing an international broadband network for satellite communications systems, and at the same time to demonstrate that satellite communications is a very practical broadband network application. It was decided to implement the High-Pre-

cision Video/Remote Post-Production Experiment proposed by the Jet Propulsion Laboratory (JPL) as the broadband network application for the experiment.

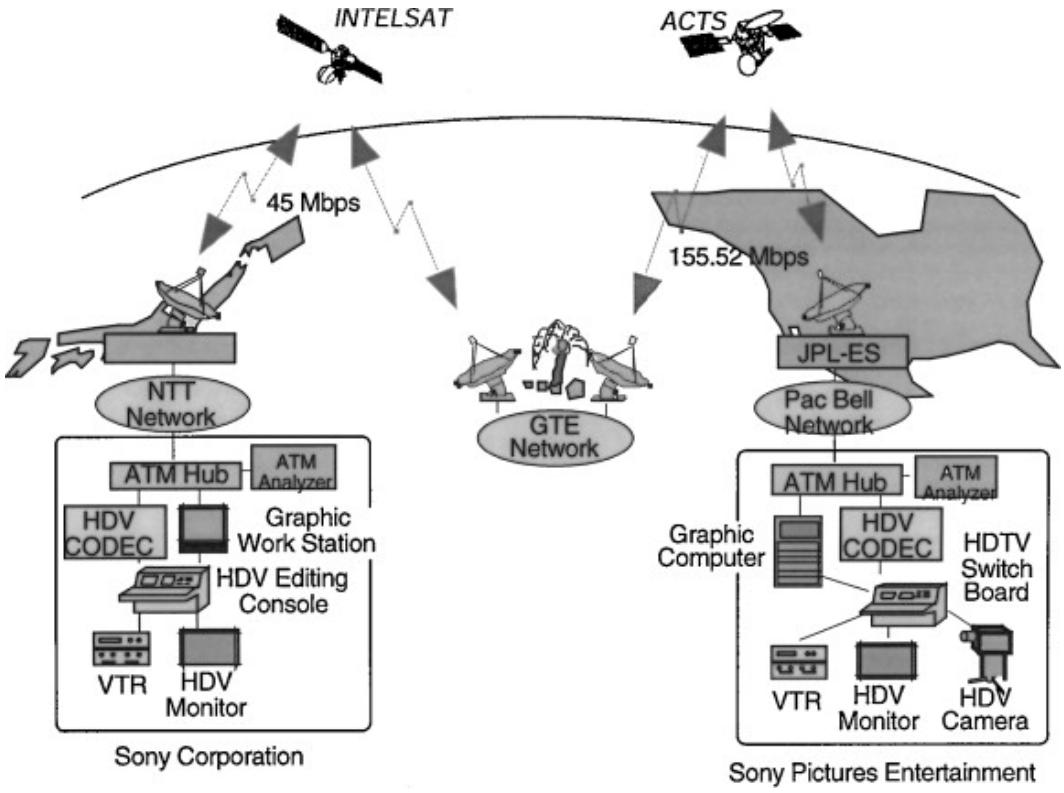

FIGURE 29. Configuration of Trans-Pacific HDR experiment.

The second phase of this experiment was conducted by using a satellite network of INTELSAT and N-STAR in July 2000. The Internet was configured to use a high-speed satellite link of 45 Mbps in this experiment, and there is originality in having realized an application to make data available to users at multiple points. In a remote astronomy distance-education demonstration, a telescope at Wilson Mountain astronomical observatory was controlled remotely from CRL, NASA/JPL, KMSI (Keck Math/Science Institute), and the University of Maryland. The telescope data was displayed in a computer at hand through a dispersion filing system via a server at NASA/ARC (Ames Research Center) and participants were enabled to utilize these data simultaneously. Pupils both of Sohka High School in Tokyo and of Crossroads School in Santa Monica experienced a virtual astronomical observation classroom. In a visible human telemedicine demonstration, data from the visible human of NLM (National Library of Medicine) was transmitted at high speed to Sapporo Medical College successfully. The information that could be transmitted in about 3 minutes conventionally was transmitted via satellite in about 10 seconds.

> Read full chapter

OBSERVATIONS PLATFORMS | Rockets

M.F. Larsen, in Encyclopedia of Atmospheric Sciences (Second Edition), 2015

Introduction

The influence of the lower atmosphere on our daily lives is immediately clear because of the weather processes that occur there. The processes that occur in the upper atmosphere are also important, although that did not become evident until the space age began at the end of World War II. As we become more dependent on space and satellite communications, as well as traditional radio communications, understanding those processes becomes critical. The ionosphere, which covers the region from approximately 80 km to altitudes above 1000 km, is a mixture of neutral gas constituents and charged particles. The plasma, as it is known, and the electrodynamic forces that drive it can produce small-scale fluctuations in the charged particle densities that can affect radio and satellite communications significantly. The temperatures, composition, and density of the neutral gas component can also have large variations in response to both local processes and changing activity on the Sun. Such effects can alter satellite and other spacecraft trajectories enough to be a concern. Measuring the properties of the atmosphere at high altitudes where the dynamical properties are both interesting and important but where the densities are low enough to make measurements difficult has been a continuing challenge, especially in the period since World War II. The measurement techniques used extensively include ground-based remote sensing with radars and optical techniques, measurements from satellites, and measurements from suborbital rockets, also known as sounding rockets. This article will focus on the techniques used to obtain measurements from the rocket platform.

The layers of the atmosphere closest to the surface of the Earth are the troposphere and stratosphere. Above 45 to 50 km altitude, where the stratosphere ends, the temperature again decreases with altitude in the layer known as the mesosphere, followed by a region of steadily increasing temperature above 90 km, known as the thermosphere, where the absorption of extreme ultraviolet radiation from the sun is primarily responsible for the temperature increase. Radiation from the Sun also leads to the ionization of neutral particles in that region which, because of the importance of the charged constituents, is also known as the ionosphere.

Between the surface of the Earth and the region near 100 km altitude, the density of the atmospheric gas decreases by a factor of approximately 1□000□000, and traditional techniques for making measurements *in situ* from platforms such as balloons or aircraft do not work, since the platforms cannot be supported by the atmosphere.

New possibilities for probing the upper-altitude regions became available at the end of World War II when rockets developed by the Germans during the war and captured by the Allies became available for scientific investigation.

> Read full chapter

GOES-R Series Data Access and Dissemination

James McNitt, ... Graeme Martin, in The GOES-R Series, 2020

22.2 Product Generation, Access, and Dissemination Framework

Fig. 22.1 describes how the GOES-R ground system operates from three NESDIS sites: NSOF, WCDAS, and the Consolidated Backup (CBU) facility. The GOES-R Series ground system consists of the following elements: mission management (MM), PG, PD, and enterprise management (EM).

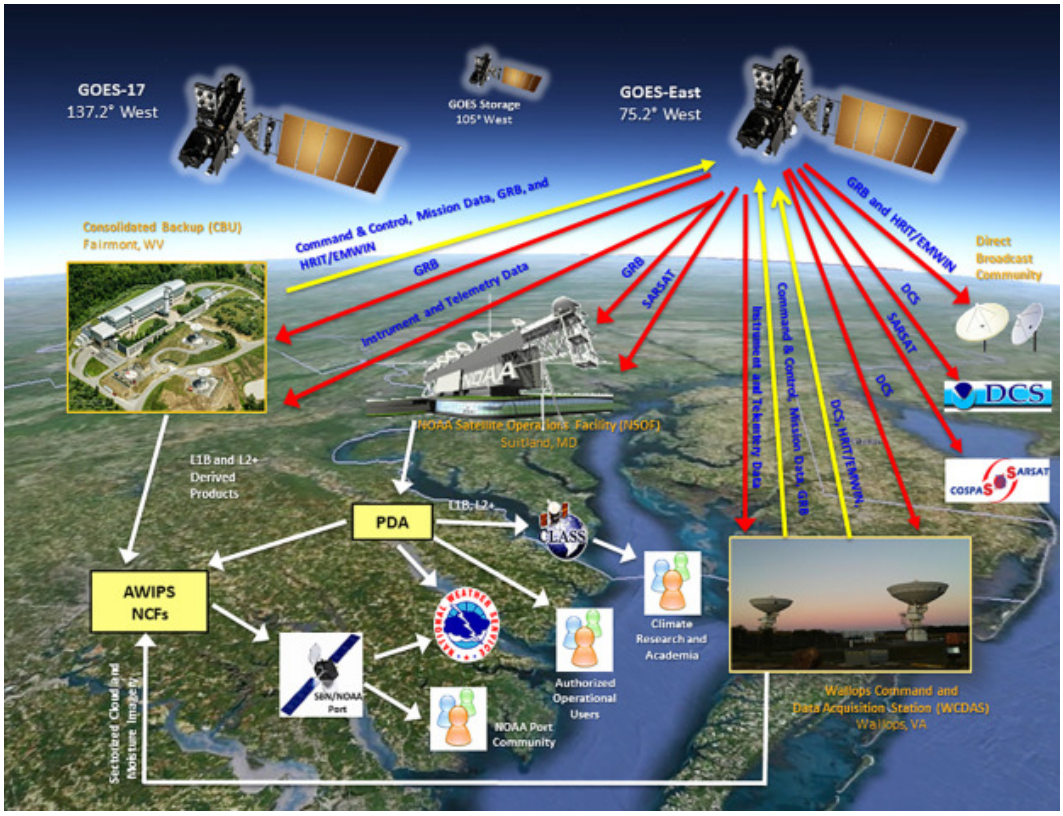

Fig. 22.1. GOES-R ground system architecture.

WCDAS hosts the primary space communications services, EM and MM functions, and selected PG and PD functions. The GOES-R Series Product Definition and Users' Guide (PUG) Volume 2 describes the Level 0 products (GOES-R Program, 2018a). The Level 0 products are composed of Consultative Committee for Space Data Systems (CCSDS) packets that contain all the science, housekeeping, engineering, and diagnostic telemetry data from the ABI, GLM, SUVI, EXIS, SEISS, and MAG instruments. The content and form of the CCSDS space packets in the Level 0 product files are exactly as generated by the instruments. The Level 0 product files also contain orbit and attitude/angular rate packets generated by the spacecraft. The type and format of each packet are indicated as a unique application process identifier (APID).

WCDAS receives all Level 0 data products, and its PG function creates Level 1b and the GLM Level 2+ products in Network Common Data Form (netCDF) format, information packets, and metadata. It also maintains Level Zero Storage Service (LZSS) access for authorized calibration/validation users. The ground system software at WCDAS then encodes the Level 1b and GLM Level 2+ products as CCSDS packets and transmits them, along with information and metadata packets, up to the satellite. The packets are relayed through the GRB transponder and L-band antenna to the ground. The GRB receive stations at NSOF and other sites receive the GRB RF stream. The PG function creates the rest of the L2 + products and distributes the Level 1b and Level 2+ products to the PD node in ESPC.

CBU functions as a completely independent backup for the MM and selected PG and PD functions for KPP and GRB PG, and it can operate concurrently with NSOF and WCDAS. Its X-band antenna receives Level 0 data and the PG function produces GRB products, information packets, and metadata that are uplinked to the satellite for relay through GRB. CBU can also generate the sectorized cloud and moisture imagery (SCMI) product for NWS.

NSOF hosts the primary MM and selected PG and PD functions and is responsible for maintaining the calibration database, monitoring radiometric and image navigation and registration (INR) performance, generating Level 2+ products, and disseminating Level 1b and Level 2+ products.

ESPC is NOAA's primary data-processing system for the nation's environmental satellite data. Through a large variety of hardware, software, networks, telecommunication lines, and software tools, ESPC ingests, processes, and distributes environmental data and information received from all of NOAA's satellites, several foreign countries' satellites, and the Department of Defense's (DoD's) satellites. PDA is the PD node in ESPC that distributes Level 1b products, Level 2+ products, and associated mission data.

Satellite RF Communications and On-board Processing

Robert C. Moore, in Encyclopedia of Physical Science and Technology (Third Edition), 2003

III Modulation

Modulation is the process of imposing base-band information onto a RF carrier for subsequent transmission. Essentially the modulation process alters the base-band information by converting it to a form that permits more efficient transmission. The information signal varies one or more characteristics of a sinusoidal RF carrier. These characteristics are amplitude, frequency, and phase.

If the carrier is represented by A cos[2π f_c + □], where A is the amplitude, f_c is the frequency, and □ is the phase angle, then modulation may be accomplished by varying A, f_c, or □ in accordance with the information message. These three types of modulation are called amplitude modulation (AM), frequency modulation (FM), and phase modulation (PM). The latter two types are examples of *angle modulation*.

III.A Linear and Digital

Linear modulation is a scheme in which the base-band signal is linearly related to the modulated signal; that is, the modulated signal reflects a continuously variable range of values of the base-band signal. Linear modulation has very limited use in space systems.

Digital modulation is a scheme in which the base-band information has first been converted to a digital message (that is, a message that assumes only one of a finite number of discrete values at a time) before modulation takes place. The digital equivalent of amplitude modulation is *amplitude shift keying* (ASK), the digital equivalent of frequency modulation is frequency shift keying (FSK), and the digital equivalent of phase modulation is phase shift keying (PSK). In satellite communications PSK is the most commonly used modulation scheme. FSK is occasionally used in applications for which receiver simplicity is a driver.

Detection of the signal from an amplitude-modulated carrier (*demodulating* the carrier) may be accomplished using a simple envelope detector. By contrast, angle modulation (FM or PM) must be demodulated by tracking the changes in frequency

or phase, using more complex electronics than those required for demodulating AM. In general, FM receivers are simpler to design than PM receivers.

Although it is easier to demodulate, an AM system is more vulnerable to signal fluctuations and noise that affects amplitude. For this reason, AM is seldom used in satellite communications. For inter-satellite (cross-link) communications; however, there is no intervening atmosphere with its propagation effects, so proposed inter-satellite links (ISLs) frequently employ optical (laser-based) communications using ASK.

To achieve the desired signal-to-noise ratio (SNR) with an FM system it is possible to trade off carrier power with bandwidth. For example, in a power-limited design the SNR may be increased by increasing the value of the frequency deviation.

With PSK, the phase of the modulated signal is changed in discrete steps, where each discrete phase value corresponds to a discrete value of the digital modulating signal. For example, the base-band signal commonly uses only two symbols (0 and 1). These symbols may be used individually to set the carrier phase to 0 or 180 ° (*bi-phase shift keying*, BPSK), or the symbols may be used in pairs to set the carrier phase to 0, 90, 180, or 270 ° (quadrature phase shift keying, QPSK). QPSK has smaller phase differences between values ($\Delta \theta = 90$ ° for QPSK, versus 180 ° for BPSK), so QPSK is more easily upset by phase noise. QPSK has one very large advantage, however, and that is its spectral efficiency. QPSK can transmit approximately 1.4 information bits/Hz of bandwidth, while BPSK can transmit only about 0.7 information bits/Hz of bandwidth. Frequently the presence of adjacent carriers places tight restrictions on usable RF bandwidth, so bandwidth efficiency can be very important to a satellite communications link design. (The bandwidth efficiency of PSK is not shared by FSK modulation, which is another reason to prefer PSK over FSK.) With both BPSK and QPSK modulation there are rapid changes of phase at the bit boundaries. These phase changes generate undesired *side-band energy* that is outside the main spectrum of the modulated signal.

Regardless of the type of modulation used, because of propagation effects and receiver noise a space communication channel will experience occasional errors. For digital modulation, these random errors are *bit errors* that will occur with a certain probability. Performance is indicated by estimating or measuring the average *bit error rate* (BER) of the RF link. For example, if a transmission has an average of *n* bit errors out of 100,000 bits transmitted, then the BER is $n \times 10^{-5}$. Notice that with this definition the BER is equal to the probability of a bit error.

For command up-links there may be two types of modulation, because the command message is first modulated onto a subcarrier (typically 16 kHz), then the modulated subcarrier is used to modulate the RF carrier. The subcarrier is used because the carrier is almost completely suppressed during transmission. The presence of

the subcarrier in the spectrum permits the satellite command receiver to lock onto the signal. Often FSK is used for the subcarrier and PSK for the carrier.

III.B Coding Methods

Channel coding is a processing method by which redundancy is added to message to mitigate the effects of message signal impairment during subsequent transmission. Redundant bits are incorporated into the base-band digital messages to protect against noise corruption or other impairment of the transmitted RF signal. Incorporation of these redundant bits is called *structured redundancy*. In the majority of satellite communication down-links, coding is applied to telemetry in such a manner that error detection and correction is possible at the ground receiver without having to resort to any feedback to the transmitter, such as requests for retransmission. This type of coding is called forward error correction. Another type of error correction is achieved by feeding back requests for retransmission to the transmitter. This coding technique is called automatic repeat request (ARQ). Closing the feedback loop for ARQ introduces time delays into the system. These delays often make ARQ unacceptable for a satellite communications system.

Coding is applied only to digital base-band messages. In applications for which error-free transmission is essential, such as the command up-link, ARQ coding techniques are used unless the command messages are lengthy (usually they are not) or the magnitude of the repeat delay is prohibitive (frequently it is). With applications for which only "nearly error-free" transmission is desired, such as down-link of mission-critical telemetry data, forward error correction is used so as to minimize the bit error rate. Regardless of the type of coding used, errors are still possible. An uncorrectable bit error in a frame of telemetry data usually results in a request to retransmit the frame.

Most practical forward error correction codes are implemented using digital shift registers and modulo-2 adders (multiple-input exclusive-OR gates). These are algebraically linear devices; the codes they implement are *linear codes*. For forward error correction, satellite systems employ two families of linear code: *block code* and convolution *code*.

III.B.1 Block Codes

A block code operates on groups of bits organized as blocks. For example, a block of n bits may comprise k information bits plus r redundancy bits, so that $n = k + r$. Such a block code is called a (n, k) code, and is said to have a *rate* of k/n. A *rate* 1/2 code ($k = r$) will generate code symbols at twice the information bit rate. A commonly used block code is the Reed–Solomon (RS) code, which is used for channels where bursts of noise (impulsive noise) are expected. The NASA standard Reed–Solomon

code ($n = 255$ $k = 223$), with an interleaving depth of 5, adds 160 bytes of redundancy to every 1115 bytes of information. This code can correct an error burst 80 bytes in length.

Although RS codes are good at correcting bursts of errors, where the bursts are separated by relatively large periods of error-free transmission, one limitation of RS codes is that they are inefficient in correcting random bit errors. For channels that exhibit both impulse noise and random noise, the RS code may be *concatenated* with another code, such as a *convolution code*, that provides correction for random bit errors. The two concatenated codes provide better error correction than either code would when used by itself.

III.B.2 Convolution Codes

A *convolution* encoder is a feed-forward device that produces code symbols continuously; it does not require assembly of a block or frame prior to encoding the information. Convolution codes are implemented using shift registers. The name derives from the method of generating the code: information bits are convolved with the impulse response of the shift register. As information bits pass through the shift register(s), modulo-2 adders (multiple-input exclusive-OR gates) are used to form coded bit streams, which are then sequentially sampled to form the encoded symbol stream. The number of bits in the shift register(s) is the *constraint length* or *span* of the code. Error correction capability and decoding complexity both increase as the span of the code is increased.

At the end of each message frame the shift register(s) must be cleared by feeding in a stream of logic zeros. This overhead makes the convolution code unsuitable for use with very short messages. Block codes are better suited to short transmissions.

III.B.3 Turbo Codes

Turbo codes are a superset of block and convolution codes in which parallel concatenation of simple codes is combined with an interleaver to generate the encoded symbol sequence. Information bits are first arranged into blocks of length N, where N is the depth of the interleaver. The interleaved information bits then pass through simple shift register encoders to generate the encoded symbol stream. For typical satellite communications, turbo codes generally out-perform concatenated RS and convolution codes. For this reason turbo codes are rapidly gaining wide acceptance for satellite down-links, and turbo decoders may be found as standard equipment at most ground stations.

III.B.4 Coding Gain

Coding gain is defined as

Here E_b is the received energy per bit (received power multiplied by the bit period), and N_o is the received noise spectral density (received noise power divided by the receiver noise bandwidth). This assumes that the uncoded and coded messages have identical bit error rates at the receiver, and that the rate of information transmission is also identical. Coding gains in the range from 4 to 8 dB are practical. Coding gain quantifies how a code will increase the link margin or reduce the transmitter power requirements. Typical desirable values for E_b/N_o range from 5 to 12 dB.

Figure 1 shows a typical plot of Eb/N_o versus probability of bit error (=BER), with and without coding. For a probability of bit error equal to 10^{-5}, BPSK without coding gives E_b/N_o = 9.6 dB. With rate–1/2, K = 7 convolution encoding, Eb/N_o = 4.4 dB, yielding a coding gain of 9.6–4.4 = 5.2 dB. Figure 1 shows that an additional coding gain of 1.8 dB may be achieved by concatenating the convolution code with a (255, 223) RS code.

FIGURE 1. Probability of bit error versus E_b/N_o for several types of coding.

Figure 1 also shows the Shannon limit (Eb/N_o = –1.6 dB) below which error-free communication cannot occur regardless of information rate or coding method. This limit derives from the *Shannon-Hartley theorem* of information theory. Turbo codes help a system approach the Shannon limit.

> Read full chapter

Communication masking in marine mammals: A review and research strategy

Christine Erbe, ... Robert Dooling, in Marine Pollution Bulletin, 2016

6.4 Habitat-wide assessments

The above steps outlined how masking can be assessed for specific spatial arrangements of caller, listener and masking noise. In the field, caller, listener and noise sources move. In an attempt to incorporate these movements into a simple model of masking, Clark et al. (2009) estimated the effect of the time-varying distribution of ships on the communication space of baleen whales. Hypothetical calling whales and listening whales were distributed uniformly across the species' habitat in this modelling effort, and actual ship positions as a function of time were used to estimate anthropogenic noise levels across the study area. Recordings of ambient noise made at the site were used to determine natural ambient conditions. Sound propagation was modelled from every caller to every listener. The volume of space over which the listeners could hear each caller in quiet conditions was compared to the reduced volume of space as multiple ships passed through the habitat simultaneously. The loss of communication space for all callers was integrated into a masking index as a function of time. This model can account for directional sources and directional hearing capabilities of the animal (via a directivity index), if this information is known for the target species. No information about directivity was available for this scenario with baleen whales. In the absence of CR information for baleen whales, Clark et al. (2009) used 1/3 octave bands combined with an equal energy hypothesis to approximate auditory processing by the whales. Equal-energy in each band determined signal detection; a higher SNR was used to model signal recognition. The outcome of this effort illustrated the potential loss of communication space in this ship noise scenario as a result of masking. However, given the lack of knowledge about hearing in mysticetes, it relied heavily on a number of assumptions.

An agent-based (animat) model (e.g., Donovan et al., 2012; Frankel et al., 2002; Mountain et al., 2013; Shyu and Hillson, 2006) can be incorporated into other habitat-wide assessments, that allow movement of callers and listeners according to behavioural rules. Such rules might include behavioural responses to noise. In theory, these models could keep track of the amount of masking each listener experiences over time. However, a large knowledge base is needed to support such a model. This includes knowledge of the propagation environment, the types of signals that are biologically relevant, the species that live in the area, the hearing capabilities of these species, their physical and acoustic behaviour etc. While some of this information is available, much is not, and for this reason, further work is needed to provide data for successful masking models for anthropogenic noise.

> Read full chapter

An overview of North Atlantic right whale acoustic behavior, hearing capabilities, and responses to sound

Leanna P. Matthews, Susan E. Parks, in Marine Pollution Bulletin, 2021

4.2.1 Vocal response to noise

North Atlantic right whales occupy coastal habitats that overlap with high levels of anthropogenic activity, which has prompted an interest in the effects of anthropogenic noise on right whale acoustic behavior. The current literature on the impacts of anthropogenic noise on acoustic behavior has generally looked at the impacts of vessel noise, as opposed to other noise sources. This is predominately due to the fact that noise from vessels is the main contributor to increased noise levels in these habitats. Compared to historically lower noise conditions from the mid-20th century, North Atlantic right whales are estimated to have lost 63–67% of their natural communication space, i.e., the amount of acoustic habitat available for signaling whales, when considering upcalls (Hatch et al., 2012). Gunshots are less impacted by increased noise levels, with an estimated decrease in communication space of only 5% (Cholewiak et al., 2018). In order to combat the effects of a decrease in communication space loss, individual callers must shift certain aspects of their signal, such as call frequency, duration, or amplitude. Acoustic propagation modeling in the Bay of Fundy has shown that increasing the start frequency and the amplitude of upcalls could increase the detection range of these signals in the presence of noise (Tennessen and Parks, 2016). The upcall in this habitat is especially important to consider, as upcalls are used in mother-calf communication and aid in reunion events (Parks and Clark, 2007). The acoustic model of Tennessen & Parks et al. (2016) mimics adjustments of frequency and amplitude of calls that have been documented in individual North Atlantic right whales.

One comparison of acoustic data from North Atlantic right whales analyzed recordings from 1956 and from the early 2000s (Parks et al., 2007b; Parks et al., 2008). This historical data, characterized by lower levels of background noise levels, was recorded off the coast of Massachusetts, while the more modern dataset was recorded in multiple habitats, including off the coast of Massachusetts and in the Bay of Fundy (Parks et al., 2007b; Parks et al., 2008). This comparison demonstrated an increase in start frequencies and end frequencies of upcalls in the more recently recorded data (Parks et al., 2007b; Parks et al., 2008).

Another comparison was also made between North Atlantic right whale upcalls, recorded near Massachusetts and in the Bay of Fundy, and Southern right whale

upcalls, recorded near Argentina (Parks et al., 2007b; Parks et al., 2008). Southern right whales inhabit an area with much lower levels of anthropogenic noise compared to North Atlantic right whales. Upcalls from the higher noise North Atlantic habitat were shown to be higher in both start and end frequency (Parks et al., 2007b; Parks et al., 2008). Both of these comparisons, historical to modern recordings and North Atlantic to Southern right whale habitats, indicate that in higher noise levels, individuals shift their vocalizations to call at a higher frequency.

To increase detection probability in the presence of noise, individual callers can also adjust the duration of vocalizations. Compared to historical data, recent recordings of North Atlantic right whales show an increase in duration and therefore an increase in the amount of acoustic information being broadcasted in the higher noise environment (Parks et al., 2007b; Parks et al., 2008).

The levels of background noise to which right whales are exposed not only vary on large temporal and geographic scales, but can also change within the primary migratory corridor for the North Atlantic right whale population or even within a single habitat area. When comparing the background noise levels in the 50–350 Hz band for the Southeast United States, Cape Cod Bay, and the Bay of Fundy, there is much a much higher level of background noise in the Bay of Fundy, with the lowest ambient noise in the Southeast United States (Parks et al., 2009). Individuals in the Bay of Fundy are also exposed to high noise levels for longer periods of time, compared to other habitats (Parks et al., 2009). The call parameters in these habitats are, as expected, also different, with higher minimum frequency for upcalls recorded in the high noise area of the Bay of Fundy (Parks et al., 2009). However, upcalls in the Bay of Fundy have a shorter duration (Parks et al., 2009). This decrease in duration in higher noise levels contrasts the increased duration seen in previous studies (Parks et al., 2007b; Parks et al., 2008), but might indicate a different strategy for acoustic compensation. Parks et al. (2009) also mention that the variation in call parameters between the habitats is minimal and could be the result of differences in acoustic propagation due to variation in physical difference in habitat. It should be noted that in all three studies discussed above (Parks et al., 2007b; Parks et al., 2008; Parks et al., 2009), data was collected via bottom mounted archival recorders. Therefore, the authors were unable to determine the age and sex classes of individual callers, which also is known to impact acoustic parameters, such as frequency and duration (Root-Gutteridge et al., 2018).

A notable vocal adjustment in the presence of noise has been demonstrated using tag data from North Atlantic right whales in the Bay of Fundy. The use of tags allowed researchers to assess how changes in background noise impact the amplitude at which calls are produced. Multiple years of data from male and female whales of various age classes revealed a linear relationship between noise level in the 20 Hz to 8 kHz band and signal level, with a higher signal amplitude in higher levels

of background noise (Parks et al., 2011b). On this individual level in one habitat, however, there was no statistically significant variation in frequency or duration parameters (Parks et al., 2011b). The lack of statistical significance was likely due to low call rates from individuals and further complicated by the fact that some individuals increased frequency in the presence of increased noise, while others decreased frequency in the presence of noise (Parks et al., 2011b).

Overall, North Atlantic right whales appear to exhibit vocal shifts in the presence of anthropogenic noise that are consistent with other mammalian species, including an increase in frequency, and change in call duration, and an increase in amplitude. This is important to consider when using automatic detectors to confirm the presence of right whales in a given habitat since variation in call parameters can decrease the effectiveness of a detector (Urazghildiiev et al., 2009).

> Read full chapter

SMART-1 technology, scientific results and heritage for future space missions

Planetary and Space Science, 2018

Abstract

ESA's SMART-1 mission to the Moon achieved record firsts such as: 1) first Small Mission for Advanced Research and Technology; with spacecraft built and integrated in 2.5 years and launched 3.5 years after mission approval; 2) first mission leaving the Earth orbit using solar power alone; 3) most fuel effective mission (60 L of Xenon) and longest travel (13 months) to the Moon!; 4) first ESA mission reaching the Moon and first European views of lunar poles; 5) first European demonstration of a wide range of new technologies: Li-Ion modular battery, deep-space communications in X- and Ka-bands, and autonomous positioning for navigation; 6) first lunar demonstration of an infrared spectrometer and of a Swept Charge Detector Lunar X-ray fluorescence spectrometer; 7) first ESA mission with opportunity for lunar science, elemental geochemistry, surface mineralogy mapping, surface geology and precursor studies for exploration; 8) first controlled impact landing on the Moon with real time observations campaign; 9) first mission supporting goals of the International Lunar Exploration Working Group (ILEWG) in technical and scientific exchange, international collaboration, public and youth engagement; 10) first mission preparing the ground for ESA collaboration in Chandrayaan-1, Chang' E1 and future international lunar exploration.

We review SMART-1 highlights and new results that are relevant to the preparation for future lunar exploration. The technology and methods had impact on space research and applications. Recent SMART-1 results are relevant to topics on: 1) the study of properties of the lunar dust, 2) impact craters and ejecta, 3) the study of illumination, 4) radio observations and science from the Moon, 5) support to future missions, 6) identifying and characterising sites for exploration and exploitation. On these respective topics, we discuss recent SMART-1 results and challenges. We also discuss the use of SMART-1 publications library. The SMART-1 archive observations have been used to support the goals of ILEWG. SMART-1 has been useful to prepare for Kaguya, Chandrayaan-1, Chang'E 1, the US Lunar Reconnaissance Orbiter, the LCROSS impact, future lunar landers and upcoming missions, and to contribute towards objectives of the Moon Village and future exploration.

> Read full chapter

Future of Space Astronomy: A global Road Map for the next decades

Pietro Ubertini, ... Mikhail Pavlinsky, in Advances in Space Research, 2012

4.3.5 INTEGRAL: International Gamma-Ray Astrophysics Laboratory

The ESA INTEGRAL mission was approved as the 2nd medium size ESA project of the Horizon 2000 scientific programme in April 1993 (see Fig. 12), (Winkler et al., 2003). The programme is led by ESA, with the instrument complement and the Scientific Data Centre (based in Geneva) provided by five different European consortia. Contributions were also provided by Russia, for the Proton launcher, and by the USA which made available the NASA Deep Space Network ground station at Goldstone.[40] The payload was calibrated at the beginning of 2002 at the European Space Research and Technology Centre (ESTEC) in Noordwijk, the Netherlands. INTEGRAL was successfully launched from Baikonur (Kazakhstan) on 17 October, 2002 for a planned operational lifetime of 2 years with possible extension. The Observatory is devoted to the observation of the □-ray Universe in the energy range from 15 keV to 10 MeV with substantial monitoring capability in the X-ray range, from 3 to 30 keV, and in the optical V band at 550 nm. The two □-ray instruments are the spectrometer, SPI, and the imager, IBIS. SPI is a high resolution, cooled, germanium-based coded mask spectrometer with unprecedented sensitivity to diffuse emission over a very wide field of view (□25° FWHM) (Vedrenne et al., 2003). It is optimised for high resolution □-ray line spectroscopy in the energy range 20 keV–8 MeV. IBIS is a large area coded

aperture mask telescope based on two layers of 16,384 Cadmium Telluride (CdTe) detectors and 4,096 Caesium Iodide (CsI) detectors (Ubertini et al., 2003). It provides fine angular resolution (<12 arc min), wide spectral response (15 keV–10 MeV), high resolution timing (60 μs) and spectroscopy (6% at 100 keV) . In view of the impossibility of focusing high energy X-rays and soft □-rays, the three high energy instruments are operated with a coded mask to provide good imaging capability over a wide field of view. Of course, the coded mask technology and "pixel" size are different for the X-ray monitor and for the two □-ray instruments.

Fig. 12. INTEGRAL during ground testing at ESTEC, ESA.

This technique is a key feature of INTEGRAL to provide simultaneous images of the whole field observed and detection and location of all the sources. It also provides the best "on-source" and "background" measurements in a time-independent manner. INTEGRAL provides almost an order of magnitude improved performance in spectroscopy and imaging compared to earlier high energy observatories, such as BeppoSAX, RXTE, GRANAT and the Compton Gamma-Ray Observatory (CGRO). On 15 January, 2010, ESA's advisory bodies approved the extension of INTEGRAL operations until 2014.

4.3.5.1 Mission achievement summary

With its broad energy range, INTEGRAL provides an astronomical bridge between the soft X-ray missions, such as XMM-Newton, Chandra, Suzaku, Swift, and NuSTAR, the space-based high-energy -ray facilities in the GeV regime, such as Fermi and AGILE, and "ground based" -ray telescopes for higher (TeV) energies, such as the The High Energy Stereoscopic System (H.E.S.S), the Major Atmospheric Gamma-ray Imaging Cherenkov Telescopes (MAGIC) and the Very Energetic Radiation Imaging Telescope Array System (VERITAS). The primary astronomical usage of the observatory is for high-resolution spectroscopy with imaging and arc min positioning of celestial sources of hard X-ray/-ray emission. High-resolution spectroscopy over the entire energy range permits spectral features to be uniquely identified and line profiles to be measured for studies of physical conditions in the source region. The high-resolution imaging capability of INTEGRAL within a large field of view permits accurate location of the high energy emitting sources and hence identification with counterparts at other wavelengths (Bazzano et al., 2006). It also enables extended regions to be distinguished from point sources and provides considerable serendipitous science, which is very important for an observatory-class mission (see Fig. 13). INTEGRAL remains unique world-wide as an observatory providing these capabilities. Key science areas of INTEGRAL include:

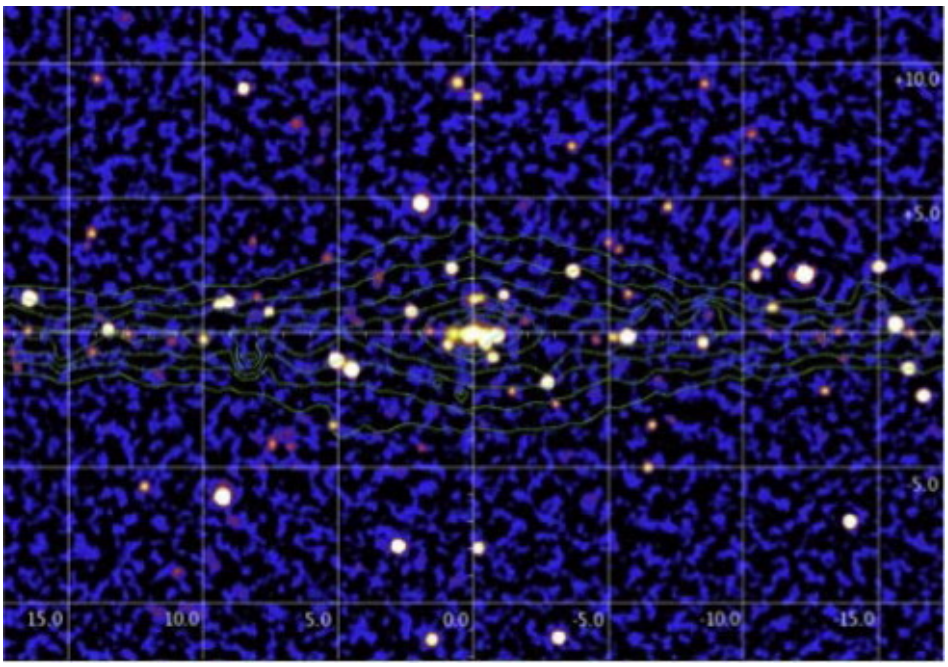

Fig. 13. The central part of the Milky Way Galaxy seen by INTEGRAL/IBIS (17–60-keV). Green curves are iso-contours of surface brightness in the infrared from COBE/DIRBE, tracing the surface density of stars in the Galaxy. The maximum sensitivity of the map is within 5–10 of the Galactic Centre. Credit: Krivonos et al., A& A 519, A107, 2010.

1. Studies of nucleosynthesis through -ray lines from elements formed in supernovae.
2. Studies of positron production and annihilation.

3. Studies of the physics of emission mechanisms of white dwarfs, neutron stars, and black holes and associated transient phenomena.
4. Deep surveys for supermassive black holes in Active Galactic Nuclei, and
5. -ray burst studies.

The main results obtained so far include the first sky map in the light of the 511 keV annihilation emission, the discovery of a new class of high mass X-ray binaries and detection of polarisation in cosmic high energy radiation. For the foreseeable future, INTEGRAL will remain the only observatory enabling the study of nucleosynthesis in our Galaxy, including the next, long overdue, nearby supernova, through high-resolution -ray line spectroscopy (Winkler et al., 2011). INTEGRAL observations have uncovered a new class of highly absorbed, slowly spinning pulsars, have shown pulsar wind nebulae to be the -ray counterpart of the new TeV sources, and detected the most distant -ray quasars, a break-trough in relativistic astrophysics. The 30% unidentified new INTEGRAL sources are a remaining mystery. Recently, the new class of Fast Supergiant X-Ray Transients has been discovered by INTEGRAL, posing a challenge to stellar evolution modeling (Sguera et al., 2005; Ubertini et al., 2006; Sidoli et al., 2007).

> Read full chapter